JOURNAL OF SOLID STATE CHEMISTRY **125,** 281–284 (1996)
ARTICLE NO. 0299

LETTER TO THE EDITOR

Structural Features of "$Ba_4Fe_4Ti_3O_{16}$" and "$Ba_{26}Fe_{20}Ti_{21}O_{98}$" as Revealed by High-Resolution Electron Microscopy

L. A. Bendersky, T. A. Vanderah, and R. S. Roth

Materials Science and Engineering Laboratory, National Institute of Standards and Technology, Gaithersburg, Maryland 20899

Communicated by J. M. Honig, July 1, 1996; accepted June 8, 1996

Preliminary results from high-resolution microscopy and electron diffraction studies of two new compounds with approximate compositions $Ba_4Fe_4Ti_3O_{16}$ (E phase) and $Ba_{26}Fe_{20}Ti_{21}O_{98}$ (M phase) are described. The compounds were found to be structurally related and exhibit two types of structural blocks. One of the blocks (H) is ordered with respect to the other by tripling within the basal hexagonal cell. Another block (P) is apparently perovskite-related. Phase E was found to have a well-ordered structure (space group either hexagonal *P*6 or trigonal *P*3), whereas phase M exhibits persistent and regularly occurring structural disorder as revealed by the presence of diffuse, continuous streaks. We suggest that the origin of this disorder is poor correlation in translation of the H blocks.

In a recent determination of subsolidus phase equilibria in the $BaO:Fe_2O_3:TiO_2$ system the existence of 16 ternary compounds was confirmed (1). Many of the compounds apparently have new, interrelated structure types with very large unit cells; elucidation of the complete structural details of these phases is therefore technically challenging and is best accomplished by the combined use of X-ray, neutron, and electron diffraction. In the present communication we report preliminary results from high-resolution electron microscopy studies of two compounds that were found (using the disappearing phase method) at approximate stoichiometries $Ba_4Fe_4Ti_3O_{16}$ (phase E) and $Ba_{26}Fe_{20}Ti_{21}O_{98}$ (phase M) (1). Using synthesis temperatures of 1250–1270°C in air and phase analysis by X-ray powder diffraction, E and M were found to be in thermodynamic equilibrium with each other (1). Crystals of E and M, obtained from an off-stoichiometric melt and a NaCl–KCl–K_2CO_3 flux, respectively, were characterized using the precession method with Zr-filtered Mo$K\alpha$ radiation. Preliminary unit cells and space groups determined from Polaroid precession photographs were used to index the X-ray powder diffraction patterns observed for the phases: E phase, hexagonal with $a = 9.9797(5)$, $c = 23.738(1)$ Å; M phase, trigonal with $a = 5.7538(3)$, $c = 61.482(4)$ Å. The magnitudes of the c parameters which are normal to the close-packed (cp) planes suggest that E is a 10-layer and M is a 26-layer structure (2–4). In the present study we will show that the two phases are structurally related and are both built from two types of structural blocks. One of the blocks is ordered with respect to the other by tripling within its basal hexagonal cell. We will also demonstrate that while the E phase has a well-ordered structure, the M phase exhibits a persistent unusual structural disorder revealed by the presence of diffuse intensity streaks.

Polycrystalline samples of E and M were prepared by solid-state reaction of $BaCO_3$, Fe_2O_3, and TiO_2 in molar ratios of 0.440 : 0.223 : 0.337 and 0.455 : 0.175 : 0.370, respectively ($BaCO_3:Fe_2O_3:TiO_2$). Before each heating, mixtures were ground, pelletized, and placed on sacrificial powder of the same composition in alumina combustion boats. A preliminary overnight calcine at 1000°C was followed by three one-week heatings at 1265°C; the attainment of equilibrium conditions was presumed when the detailed X-ray powder diffraction patterns exhibited no further changes. Samples for electron microscopy were prepared by crushing the samples with an agate mortar and pestle. Crushed fragments were mixed with acetone and deposited onto a copper grid covered with holey carbon film. TEM specimens were examined for high-resolution imaging in a JEOL JEM-3010UHR electron microscope having a 420-nm Scherzer defocus, and for electron diffraction in a Philips 430 microscope.[1] High-resolution images were recorded with a CCD camera and analyzed using Gatans' *Digital Micrograph* software package. The analysis included fast Fourier transform (FFT) and image filtering.

[1] Certain commercial equipment is identified in order to adequately specify the experimental procedure; recommendation or endorsement by the National Institute of Standards and Technology is not therein implied.

0022-4596/96 $18.00

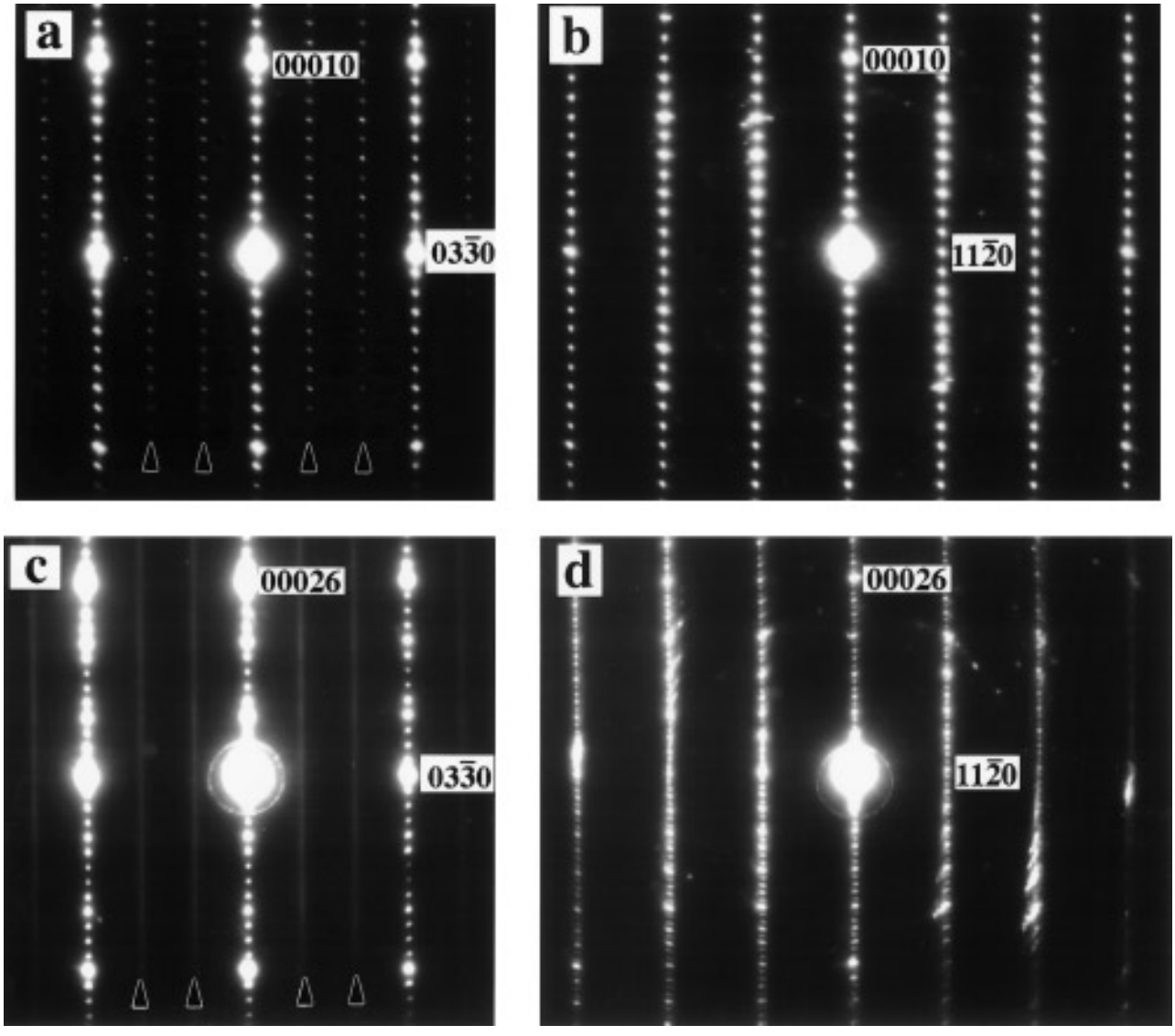

FIG. 1. SAD patterns obtained by rotating a thin crystal of E (a,b) and M (c,d) around a (000*l*) row of reflections. The angle of rotation between the patterns shown for each compound is about 30°. The patterns are indexed as the $\langle 2\bar{1}\bar{1}0\rangle$ (for a,c) and $\langle 1\bar{1}00\rangle$ (for b,d) zone axes. The arrows in (c) indicate the location of diffuse streaks, indicating regular disorder in M.

A series of selected area electron diffraction (SAD) patterns were obtained by tilting a TEM specimen around the *c* axis (most dense row of reflections). Major SAD patterns for both phases are shown in Fig. 1. The patterns for each phase are rotated about 30° from each other, consistent with the presence of either a three- or sixfold symmetry axis along $\langle 000l\rangle$; in addition, sixfold symmetric [0001] SAD patterns are observed for both phases. The *d*-spacings of the (0001) reflections, 23.7 Å for E and 61.5 Å for M, are in accord with the results obtained by X-ray diffraction (1), whereas the *a* parameter obtained for M differs: rows of weaker intensity reflections are observed at the 1/3 and 2/3 positions (indicated by arrows in Fig. 1a for E and Fig. 1c for M) between 0 and the reflection which would be indexed as $(11\bar{2}0)$ for a lattice with $a \approx 5.75$ Å. The rows are sharp reflections for the E phase and diffuse streaks for the M phase: the latter were not observed in single-crystal X-ray precession photographs of M. From the SAD results we conclude that for the M phase, $a = \sqrt{3}a_{\text{X-ray}} \approx 9.95$ Å; thus, the actual *a* parameters for E and M are approximately the same. Our results indicate that the Bravais lattice for E is hexagonal/trigonal; however, the disorder of the M phase precludes a similar conclusion based only on the SAD patterns. Nevertheless, the SAD patterns in Fig. 1 for both phases are indexed as the $\langle 2\bar{1}\bar{1}0\rangle$ and $\langle 1\bar{1}00\rangle$ zone axes.

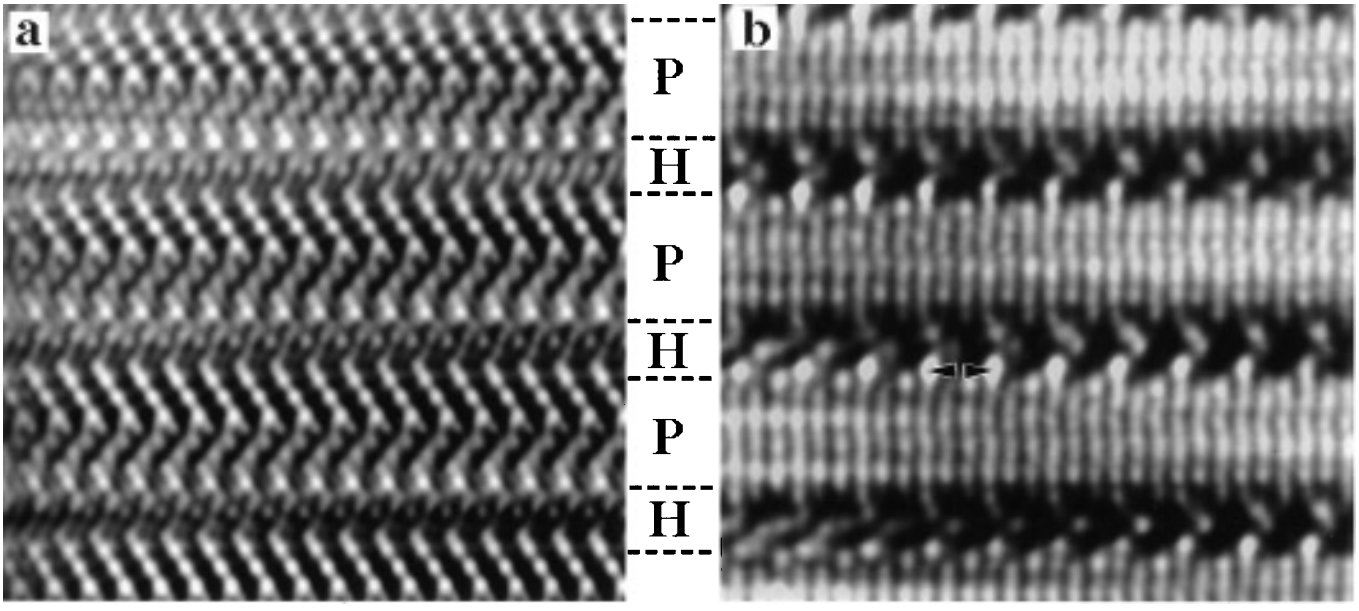

FIG. 2. HRTEM images of E taken in the $\langle 1\bar{1}00\rangle$ (a) and $\langle 2\bar{1}\bar{1}0\rangle$ (b) orientations. The images are a filtered reconstruction of the FFT of the original (a) CCD and (b) plate-recorded images.

The patterns obtained for E indicated no extinction of reflections; thus no screw axes or glide mirrors exist between symmetry elements of its space group. The possible space groups are hexagonal $P6$, $P\bar{6}$, $P6/m$, $P622$, $P6mm$, $P\bar{6}m2$, $P\bar{6}2m$, $P\bar{6}m2$, $P6/mmm$; and trigonal $P3$, $P\bar{3}$, $P312$, $P321$, $P3m1$, $P31m$, $P\bar{3}1m$, $P\bar{3}m1$. Owing to difficulties in the precise alignment of a specimen with a very large unit cell, convergent beam (CB) electron diffraction patterns did not permit definite conclusions on the overall symmetry. The $\langle 2\bar{1}\bar{1}0\rangle$ and $\langle 1\bar{1}00\rangle$ CB patterns both exhibited sym-

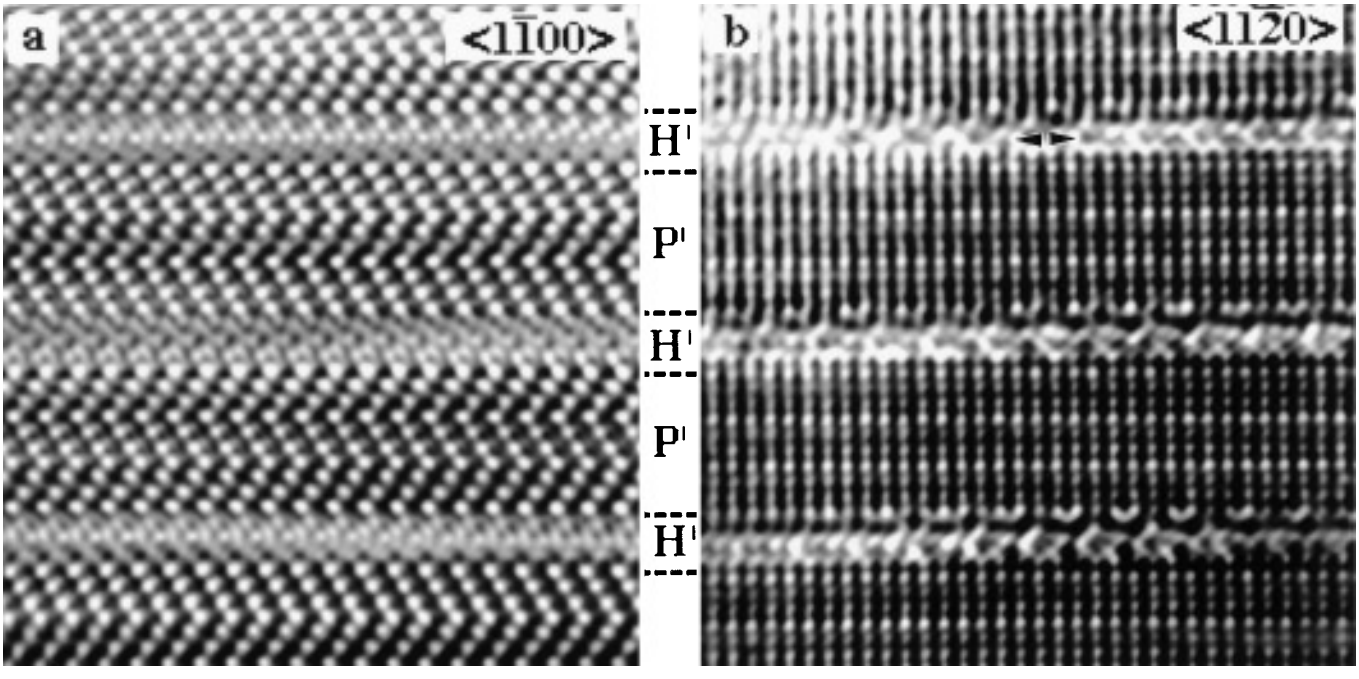

FIG. 3. HRTEM images of M taken in the $\langle 1\bar{1}00\rangle$ (a) and $\langle 2\bar{1}\bar{1}0\rangle$ (b) orientations. The images are a filtered reconstruction of the FFT of the original CCD recorded images.

metries very close to 2*mm*. However, the projected symmetries of high-resolution images, shown in Fig. 2, indicate that both the $\langle 1\bar{1}00\rangle$ and $\langle 2\bar{1}\bar{1}0\rangle$ orientations have no higher than $p11m$ projection symmetry, i.e., only a mirror plane normal to the *c* axis. (Symmetry $p2gm$ could also be considered for the $\langle 1\bar{1}00\rangle$ orientation but the presence of a glide plane was ruled out by the extinction rule.) Assuming a projection symmetry of $p11m$, the possible space groups for E are hexagonal $P6$ and trigonal $P3$. The high-resolution images for E shown in Fig. 2 suggest that its structure is built from two different blocks, denoted here as P and H. The P block has a ''herringbone'' appearance in the $\langle 1\bar{1}00\rangle$ orientation with a thickness corresponding to 7 cp layers, whereas the thickness of the H block is 3 cp layers. The high-resolution image in the $\langle 2\bar{1}\bar{1}0\rangle$ orientation (Fig. 2b) indicates that the tripling of the *a* parameter within the basal plane occurs only in the H block and not throughout the entire unit cell.

High-resolution images of the M phase taken in the $\langle 1\bar{1}00\rangle$ and $\langle 2\bar{1}\bar{1}0\rangle$ orientations are shown in Fig. 3; the corresponding SAD patterns are given in Figs. 1c and 1d. Similar to the E phase, the structure of the M phase apparently also consists of two types of blocks denoted as P′ and H′. As seen in Fig. 3, the 61.5-Å unit cell consists of two pairs of blocks, P′ + H′, where the pairs are twin-related. The P′ block in the $\langle 1\bar{1}00\rangle$ image appears as a double zig-zag row of 10 dots (''double-herringbone'') with a thickness corresponding to 10 cp layers. High-resolution image simulation of known perovskite-related structures (5) suggests that both the P and P′ blocks derive from that structural family, with different sequencing of cp layers. The H′ block appears to be very similar to the H block of the E phase; i.e., its thickness corresponds to 3 cp layers and its lateral periodicity in the $\langle 2\bar{1}\bar{1}0\rangle$ projection is three times that of the P′ block. An analysis of translation of the H′ blocks (with respect to each other) in the (0001) plane indicated that spatial correlation between the H′ blocks was poor, resulting in the observed one-dimensional disorder and observation of 1/3 and 2/3 diffuse streaks rather than well-defined spots. This interesting and regularly occurring disorder was consistently observed in other grains of M in the same preparation and in other preparations containing this phase. Further, the HRTEM images and diffraction patterns for M were essentially unaffected after the following heat treatments in air: (1) 850°C for 65 h followed by quenching in water, (2) 1275°C for 30 h followed by quenching in water, and (3) 1275°C for 50 h followed by slow cooling (3°/h) to 500°C followed by air quenching. Thermogravimetric analysis of M in flowing dry air to 900°C indicated no significant weight changes, thus ruling out oxygen intercalation (upon $Fe^{3+} \rightarrow Fe^{4+}$, as observed in the high-BaO portion of the $BaO : Fe_2O_3 : TiO_2$ phase diagram (1) as a possible cause of intralayer disorder.

Further characterization of these interesting phases is in progress including single-crystal structure determinations, neutron powder diffraction studies, and measurement of magnetic and dielectric properties.

ACKNOWLEDGMENTS

The authors thank J. M. Loezos and M. K. Rollins for assistance in sample preparation, and R. S. Gates for performing the TGA analysis.

REFERENCES

1. T. A. Vanderah, J. M. Loezos, and R. S. Roth, *J. Solid State Chem.* **121,** 38 (1996).
2. T. Negas, R. S. Roth, H. S. Parker, and D. Minor, *J. Solid State Chem.* **9,** 297 (1974).
3. R. S. Roth, L. D. Ettlinger, and H. S. Parker, *J. Solid State Chem.* **68,** 330 (1987).
4. R. S. Roth, C. J. Rawn, C. G. Lindsay, and W. Wong-Ng, *J. Solid State Chem.* **104,** 99 (1993).
5. J. Akimoto, Y. Gotoh, and Y. Osawa, *Acta Crystallogr. C* **50,** 160 (1994).